Received: 13 January 2022 | Revised: 18 May 2022 | Accepted: 22 May 2022

DOI: 10.1002/hbm.25969

RESEARCH ARTICLE

WILEY

Early alterations in cortical morphology after neoadjuvant chemotherapy in breast cancer patients: A longitudinal magnetic resonance imaging study

Xiaoyu Zhou[1] | Yong Tan[1] | Hong Yu[1] | Jiang Liu[1] | Xiaosong Lan[1] | Yongchun Deng[2] | Feng Yu[2] | Chengfang Wang[1] | Jiao Chen[1] | Xiaohua Zeng[2] | Daihong Liu[1] | Jiuquan Zhang[1]

[1]Department of Radiology, Chongqing University Cancer Hospital, School of Medicine, Chongqing University, Chongqing, China

[2]Breast Center, Chongqing University Cancer Hospital, School of Medicine, Chongqing University, Chongqing, China

Correspondence
Daihong Liu and Jiuquan Zhang, Department of Radiology, Chongqing University Cancer Hospital, School of Medicine, Chongqing University, 400030 Chongqing, China.
Email: liudaihong121@163.com and zhangjq_radiol@foxmail.com

Funding information
National Natural Science Foundation of China, Grant/Award Number: 82071883; Graduate Research and Innovation Foundation of Chongqing, China, Grant/Award Number: CYS21071; Chongqing Natural Science Foundation, Grant/Award Numbers: cstc2021jcyj-msxmX0313, cstc2021jcyj-msxmX0319; Chongqing Medical Research Project of Combination of Science and Medicine, Grant/Award Number: 2021MSXM035; 2020 SKY Imaging Research Fund of the Chinese International Medical Foundation, Grant/Award Number: Z-2014-07-2003-24

Abstract

There is growing evidence that chemotherapy may have a significant impact on the brains of breast cancer patients, causing changes in cortical morphology. However, early morphological alterations induced by chemotherapy in breast cancer patients are unclear. To investigate the patterns of those alterations, we compared female breast cancer patients ($n = 45$) longitudinally before (time point 0, TP0) and after (time point 1, TP1) the first cycle of neoadjuvant chemotherapy, using voxel-based morphometry (VBM) and surface-based morphometry (SBM). VBM and SBM alteration data underwent correlation analysis. We also compared cognition-related neuropsychological tests in the breast cancer patients between TP0 and TP1. Reductions in gray matter volume, cortical thickness, sulcal depth, and gyrification index were found in most brain areas, while increments were found to be mainly concentrated in and around the hippocampus. Reductions of fractal dimension mainly occurred in the limbic and occipital lobes, while increments mainly occurred in the anterior and posterior central gyrus. Significant correlations were found between altered VBM and altered SBM mainly in the bilateral superior frontal gyrus. We found no significant differences in the cognition-related neuropsychological tests before and after chemotherapy. The altered brain regions are in line with those associated with impaired cognitive domains in previous studies. We conclude that breast cancer patients showed widespread morphological alterations soon after neoadjuvant chemotherapy, despite an absence of cognitive impairments. The affected brain regions may indicate major targets of early brain damage after chemotherapy.

KEYWORDS
breast cancer, cognitive impairment, cortical morphology, magnetic resonance imaging, neoadjuvant chemotherapy

1 | INTRODUCTION

According to the Global Cancer Statistics 2020 report, female breast cancer has become the most commonly diagnosed cancer in the world (Sung et al., 2021). Although incremental improvements in outcomes have been obtained, cognitive problems are regularly reported in breast cancer patients who are treated with chemotherapeutic agents (Lange et al., 2019). Therefore, exploring the mechanism of cognitive impairment associated with chemotherapy in breast cancer patients is of great significance for early prevention and intervention.

Memory, attention, processing speed, and executive function are the cognitive domains vulnerable to chemotherapy (Lange et al., 2019; Wefel et al., 2015). Previous longitudinal studies have shown that breast cancer patients treated with chemotherapy have more cognitive complaints in those four domains six months (Janelsins et al., 2017) or one year after chemotherapy, particularly in working memory and executive function (Ganz et al., 2013). Notably, the aforementioned cognitive impairment develops with the detrimental effects of chemotherapy on the central nervous system, including white matter integrity (Matsos et al., 2017) and gray matter structures (Niu et al., 2021). In addition, central neurotoxicity resulting from chemotherapy may have an acute, subacute, or delayed course (Taillibert et al., 2016). However, previous studies usually focused on the subacute or delayed stages.

Neuroimaging studies in chemotherapy-exposed breast cancer patients have begun to elucidate patterns of alterations in cerebral structure and function. Cross-sectional studies have reported gray matter volume (GMV) or density attenuation in breast cancer patients at approximately 1 week (Li et al., 2018), 1 year (Inagaki et al., 2007), and even 10 (de Ruiter et al., 2012) and 20 years (Koppelmans et al., 2012) after completion of postoperative chemotherapy. Cognitive impairment in breast cancer patients was found in the above studies, while the altered brain regions varied at different time points. A study found no differences in the GMV of breast cancer patients 3 years after chemotherapy compared with patients who never received chemotherapy (Inagaki et al., 2007). Given this disagreement, longitudinal studies are necessary to detect cerebral alterations. Two longitudinal studies found gray matter density reduction in breast cancer patients from baseline to 1 month after postoperative chemotherapy completion in brain regions involving the left frontal lobes (McDonald et al., 2013a), as well as the left anterior cingulate gyrus, right insula, and left middle temporal gyrus (Chen et al., 2018). Three other longitudinal studies found that chemotherapy-exposed patients displayed wide gray matter loss 1 month after postoperative chemotherapy completion and partially recovered 1 year later, with alterations persisting predominantly in the frontal and temporal lobes (Lepage et al., 2014; McDonald et al., 2010) as well as the right lingual gyrus (Perrier et al., 2020). In addition, longitudinal studies on the white matter structure of breast cancer patients found decreases in fractional anisotropy (FA) in the frontal, parietal, and occipital white matter tracts 3–4 months after postoperative chemotherapy completion (Deprez et al., 2012) and recovered 3–4 years later (Billiet et al., 2018). These altered FA values were correlated with performance changes in attention and verbal memory. A similar trend over time was found in longitudinal studies on the brain function of breast cancer patients. Under the n-back task, breast cancer patients showed decreased frontal hyperactivation at 1 month after postoperative chemotherapy completion and partially recovered 1 year later (McDonald et al., 2012). The above alterations in cerebral structure and function suggest that there is a dynamic change over time in the brains of breast cancer patients receiving chemotherapy. Generally, the short-term time point of the previous studies was set as 1 week or 1 month after the completion of the whole chemotherapy cycles (Lepage et al., 2014; Li et al., 2018; McDonald et al., 2010). In the present study, we were interested in the early cortical morphology change pattern of breast cancer patients receiving chemotherapy for the first cycle.

In most studies of breast cancer patients receiving chemotherapy, gray matter structural properties were analyzed by the voxel-based morphometry (VBM) analysis. Beyond volume and density measured by VBM analysis, other structural properties of gray matter, including cortical thickness (CT), sulcal depth (SD), gyrification index (GI), and fractal dimension (FD), have been widely applied to cognitive domains of healthy adults (Mustafa et al., 2012; Paulus et al., 2019; Riccelli et al., 2017) and patients (Matsuda & Ohi, 2018; Pantoni et al., 2019; Wang et al., 2021) by surface-based morphometry (SBM) analysis. SBM is less susceptible to partial volume effects than VBM (Clarkson et al., 2011). Among the SBM parameters, CT is defined as the distance between corresponding points on the pial and white matter boundaries of the neocortex, and it can detect focal cortical atrophy (Fischl & Dale, 2000). A reduction in CT is thought to be associated with impaired cognitive performance in neurodegeneration (Huang et al., 2021). SD is based on the Euclidean distance between the outer and pial surfaces (Yun et al., 2013). Shallower SD can be sensitive to the detection of mild cognitive impairment and is associated with decreased CT (Im et al., 2008). GI is based on the absolute mean curvature to evaluate cortical folding (Luders et al., 2006). A lower GI is regarded as a potential marker for cognitive decline (Lamballais et al., 2020). After concurrent adjustment for cortical surface area or thickness, associations between GI and cognition remain. This suggests an independence between GI and the other measures. Thought to be associated with intelligence, FD reflects an elaborate mathematical measure that provides a quantitative description of cortical complexity (Im et al., 2006) and its reduction can serve as a sensitive marker of traumatic brain injury (Rajagopalan et al., 2019). SBM features may be promising stable markers of neural disturbance (Damme et al., 2019). To our knowledge, comprehensive SBM characteristics have not been previously reported in breast cancer patients undergoing chemotherapy.

In the present study, we hypothesized that chemotherapy can cause cerebral cortex alterations in the short term. Unlike the recruitment of breast cancer patients after surgery in previous studies, breast cancer patients receiving neoadjuvant chemotherapy before surgery were recruited in this study to avoid the confounding effects of anesthesia and surgery (Sato et al., 2015). For this longitudinal study, the first cycle completion (3 weeks after initial chemotherapy,

on average) was set as the follow-up time point, which earlier than any of the previous similar studies. With voxel-based and surface-based cortical morphology analyses, this study aimed to provide comprehensive insights into the neurological mechanism of chemotherapy-related cognitive impairment using neuroimaging.

2 | MATERIALS AND METHODS

2.1 | Participants

This prospective longitudinal study included 45 women who were newly diagnosed and pathologically confirmed to have breast cancer at Chongqing University Cancer Hospital in the first half of 2021. All participants were stage II or III breast cancer patients scheduled for neoadjuvant chemotherapy before surgery. Another inclusion criterion was right-handedness. Participants with one of the following conditions were excluded: (a) brain structural abnormalities including tumors, metastases, trauma, or a history of brain surgery; (b) a history of addiction, neurologic disorders or psychiatric disorders; (c) hormonal therapy; (d) poor quality of imaging due to metal implants or motion; (e) claustrophobia; and (f) inability to complete the subsequent magnetic resonance imaging (MRI) examination. Written informed consent was obtained from all participants according to the Declaration of Helsinki under a protocol approved by the Ethics Committee of Chongqing University Cancer Hospital.

All participants were assessed and imaged during the same days before (time point 0, TP0) and after (time point 1, TP1) the first cycle of neoadjuvant chemotherapy. Demographic information of the study participants was obtained through a self-report questionnaire and medical record abstraction. To explore the possible influence of age and treatment on cortical morphology, we divided the breast cancer patients into subgroups in post-hoc analyses. According to the median age of the patients in this study, the younger subgroup was set as age ≤ 51 years old, and the older subgroup was set as age > 51 years old. For different treatment, subgroup A was set as patients undergoing classical anthracycline-based chemotherapies, and subgroup PB was set as patients undergoing chemotherapy combined with targeted therapy.

2.2 | Neuropsychological assessment

To ensure the coherence of results, one trained psychologist made assessments by timekeeping and scoring throughout this study. Under the guidance of the psychologist, subjects underwent cognitive status assessments with a battery of neuropsychological tests in a fixed order before and after the first cycle of neoadjuvant chemotherapy. Major cognitive subdomains were tested by the following three methods: the digit span test (forward and backward) for short-term auditory memory and working memory (Hirayama et al., 2014); the trail making test (TMT; Part A) for executive function and processing speed (Bowie & Harvey, 2006); and the verbal fluency test for attention-shifting, executive function and semantic memory (Henry et al., 2004). The overall cognitive level was tested by the functional assessment of cancer therapy-cognitive function (FACT-Cog) (Version 3, simplified Chinese version). The FACT-Cog is designed for cancer patients 18 years and older with chemotherapy-related cognitive impairment based on four aspects: perceived cognitive impairments, comments from others, perceived cognitive abilities, and impact on quality of life. For the TMT, higher scores (taking more time) reveal greater impairment, while the opposite is true for the rest of the battery of neuropsychological tests. In addition, the self-rating anxiety scale (SAS) and self-rating depression scale (SDS) were used to assess anxiety and depression at TP0. According to the exclusion criteria, subjects with SAS scores >70 (major anxiety disorder) and SDS scores >73 (major depressive disorder) were excluded.

2.3 | MRI data acquisition

The MRI examinations were performed using a 3.0 T scanner (Magnetom Prisma; Siemens Healthcare, Erlangen, Germany) equipped with a 64-channel head–neck coil. Subjects were instructed to close their eyes, stay awake, and avoid thinking about any topics. Earplugs and cushions were used to alleviate the influence of noise and restrict head motion, respectively. The three-dimensional magnetization prepared rapid gradient echo sequence was used for T1-weighted acquisition with the following parameters: repetition time = 2100 ms, echo time = 2.26 ms, flip angle = 8°, field of view = 256 × 256 mm^2, matrix = 256 × 256, slice thickness = 1 mm with no slice gap, and slices = 192. The total scanning time was 4 min and 53 s. Additionally, routine axial T2-weighted images were obtained to exclude subjects with major white matter changes, cerebral infarction, or other lesions, as demonstrated by the above exclusion criteria.

2.4 | MRI data preprocessing and analyses

For the MRI data analysis, the Statistical Parametric Mapping analysis package (SPM12 version 6225; https://www.fil.ion.ucl.ac.uk/spm) and the computational anatomy toolbox (CAT12 version vcat12.7; http://dbm.neuro.uni-jena.de/cat/) implemented in SPM12 were used for VBM (i.e., GMV) and SBM (i.e., CT, SD, GI and FD) analyses. All of the procedures (http://www.neuro.uni-jena.de/cat12/CAT12-Manual.pdf) were conducted using default settings. According to the manual of CAT12, longitudinal preprocessing in CAT12 can detect more subtle effects over shorter periods of time than VBM8 in SPM12. This advantage made CAT12 more suitable for our study.

To ensure high-data quality, all original images were subjected to visual inspection, and further data quality assurance was conducted by examining the sample homogeneity of individual surfaces. As part of the longitudinal preprocessing, an initial intrasubject rigid registration was applied to realign images at two time points, and an intrasubject bias correction was applied. Images were denoised and

corrected for intensity nonuniformities, followed by segmentation into gray matter, white matter, and cerebrospinal fluid. Then, normalization was performed to the Montreal Neurological Institute space using the Diffeomorphic Anatomic Registration Trough Exponentiated Lie algebra algorithm.

For the VBM analysis, modulation was used to convert the voxel values into volume. The modulated gray matter images were smoothed using a Gaussian kernel with a full width at half maximum (FWHM) of 8 mm. After the extraction of surface parameters, SBM data were resampled and smoothed using a 15 mm FWHM for CT and a 20 mm FWHM for GI, SD, and FD. The FWHM was set according to the recommendations of the CAT12 manual. The estimated value was compared using a paired *t*-test between TP0 and TP1. Specifically, a flexible factorial design was used with conditions marked "1 2" for the image at TP0 and TP1 of each participant. Of note, covariates that do not change over time are not recommended in the longitudinal study. Therefore, no covariates were used in the general linear model in either VBM or SBM models. The statistical threshold was set at a peak-level familywise error rate (FWE)–corrected value of $p < .05$, with a cluster extent threshold of 50 voxels/vertexes. At the same time, the surviving clusters without a cluster extent threshold were explored in the Supporting Information. Anatomical automatic labeling was used for VBM, and the Desikan-Killiany atlas was used for SBM to extract mean values from preprocessed images. The extracted values with significant differences were used for subsequent correlation analysis.

2.5 | Clinical data analyses

SPSS 25.0 was used to analyze the clinical data. First, the Shapiro–Wilk test was used to verify the normal distribution of the data. Then, for the comparison of neuropsychological test scores between TP0 and TP1, a paired *t*-test was used to analyze the data conforming to a normal distribution, and the Wilcoxon signed-rank test was used to analyze the data with a nonnormal distribution. In addition, the tests that showed significant changes in longitudinal performance were selected for correlation analysis with the imaging data. Finally, correlation analyses were conducted between the longitudinal changes (calculated as extracted image value at TP1 minus that at TP0) in the VBM data and those in the four indices of SBM data in the same brain regions that survived the paired *t*-test in chemotherapy-treated patients. According to the distribution type of the data, Pearson correlation was used for data with a normal distribution, and Spearman correlation was used for data with a nonnormal distribution. Due to the exploratory nature of this analysis, multiple comparisons correction was not used.

In post-hoc analyses, longitudinal changes in brain regions which showed significant alterations (FWE $p < .05$ with a cluster extent threshold of 50 voxels/vertexes) after neoadjuvant chemotherapy were compared between subgroups. Then, to explore the possible effect of cortical morphology at baseline, the differences at TP0 were compared in those subgroups with significant longitudinal cortical changes. The two-sample *t*-test or the Wilcoxon signed-rank test was used according to data distribution.

3 | RESULTS

Of the 71 breast cancer patients who were initially recruited for the study, 18 patients changed their therapeutic schedule after baseline scanning, five patients had brain metastasis detected during the study period, one patient had a megascopic artifact due to artificial teeth, one patient had a history of schizophrenia, and one was left-handed. Among the remaining 45 patients who were enrolled for our study analysis, two patients refused the neuropsychological test at TP0, four patients refused the neuropsychological test at TP1, and six patients refused the neuropsychological test at both TP0 and TP1; however, they all agreed to MRI data collection and analysis. Therefore, the final sample sizes for the longitudinal analysis were 45 patients for MRI analysis and 33 patients for neuropsychological test analysis.

3.1 | Demographic characteristics and clinical data

All participants were women aged between 29 and 68 years old. The mean number of days between MRI scanning at TP0 and the initial receipt of the first cycle of neoadjuvant chemotherapy was 6.16 ± 4.71 days. The mean number of days between the initial receipt of the first cycle of neoadjuvant chemotherapy and MRI scanning at TP1 was 21.80 ± 3.99 days. The mean number of days between TP0 and TP1 was 27.96 ± 5.88 days. The demographic and clinical characteristics of all patients, the subgroup of patients who underwent both MRI examinations and neuropsychological tests and the subgroups divided by age and treatment are detailed in Table 1.

3.2 | Neuropsychological tests comparison

As shown in Table 2, no significant differences were observed in neuropsychological test results between TP0 and TP1. Therefore, correlation analysis with the imaging data was not adopted.

3.3 | Cortical morphology

After the first cycle of neoadjuvant chemotherapy, breast cancer patients showed a reduction in GMV in the bilateral frontal, bilateral parietal, right temporal lobes and the right rolandic operculum, whereas an increase in GMV was found in the left thalamus, hippocampus and parahippocampal gyrus (peak-level FWE-corrected $p < .05$, cluster extend threshold of 50 voxels/vertexes) (Figure 1, Table 3).

Similarly, SBM also showed significant differences between the two time points. Compared to TP0, breast cancer patients at TP1 showed CT reductions in the right superior frontal gyrus, precentral

TABLE 1 Demographic and clinical characteristics

	All patients	Patients underwent both MRI and neuropsychological tests	Subgroups divided by age			Subgroups divided by treatment		
			Younger subgroup	Older subgroup	*p* value	Subgroup A	Subgroup PB	*p* value
Demographics								
Number of participants	45	33	21	24		27	16	
Age	50.47 ± 9.08 (29–68)	50.97 ± 8.95 (29–68)	42.90 ± 6.94 (29–51)	57.08 ± 4.25 (52–68)	<.001*	49.96 ± 7.94 (30–64)	50.25 ± 10.57 (29–65)	.920
Years of education	9.29 ± 4.09 (0–16)	8.94 ± 3.82 (1–16)	10.62 ± 3.53 (6–16)	8.13 ± 4.26 (0–16)	.032*	9.44 ± 4.33 (0–16)	9.25 ± 3.98 (0–16)	.917
BMI	24.46 ± 3.70 (18.37–35.76)	23.90 ± 3.17 (18.37–31.04)	23.21 ± 2.86 (19.47–29.21)	23.90 ± 3.17 (18.37–31.04)	.024*	24.89 ± 2.99 (19.91–30.39)	24.21 ± 4.65 (19.47–35.76)	.274
Systolic blood pressure (mmHg)	123.82 ± 15.62 (100–157)	126.15 ± 15.83 (102–157)	121.47 ± 13.07 (102–154)	125.79 ± 17.59 (100–157)	.459	128.26 ± 15.93 (103–157)	114.94 ± 11.43 (100–138)	.006*
Diastolic blood pressure (mmHg)	79.60 ± 10.27 (60–99)	81.09 ± 10.05 (60–99)	80.10 ± 9.69 (63–98)	79.17 ± 10.95 (60–99)	.537	80.70 ± 10.96 (60–99)	75.94 ± 7.69 (60–89)	.129
Anxiety SAS at TP0	29.89 ± 6.32 (25–51)	30.21 ± 6.53 (25–51)	29.37 ± 6.88 (25–51)	28.22 ± 3.26 (25–51)	.077	28.70 ± 4.28 (25–43)	32.83 ± 8.88 (25–51)	.119
Depression SDS at TP0	29.13 ± 6.87 (25–60)	29.39 ± 7.17 (25–60)	30.00 ± 9.10 (25–60)	28.22 ± 3.26 (25–37)	.386	28.39 ± 7.63 (25–60)	30.75 ± 5.69 (25–45)	.031*
Menstruation, No. (%)								
Before menopause	18 (40.00%)	11 (33.33%)	15 (71.43%)	3 (12.50%)	<.001*	14 (51.85%)	4 (25.00%)	.084
Menopause	27 (60.00%)	22 (66.67%)	6 (28.58%)	21 (87.50%)		13 (41.15%)	12 (75.00%)	
Interval time								
Days from TP0 to initiation of neoadjuvant chemotherapy	6.16 ± 4.71 (0–18)	6.45 ± 4.53 (0–18)	6.38 ± 5.19 (0–18)	5.96 ± 4.36 (2–18)	.864	7.19 ± 472 (2–18)	4.50 ± 4.55 (0–18)	.040*
Days from neoadjuvant chemotherapy to TP1	21.80 ± 3.99 (15–42)	21.55 ± 2.66 (15–29)	22.33 ± 4.79 (19–42)	21.33 ± 3.16 (15–29)	.481	21.67 ± 3.01 (15–29)	22.13 ± 5.52 (18–42)	.619
Days from TP0 to TP1	27.96 ± 5.88 (20–43)	28.00 ± 5.27 (20–40)	28.71 ± 6.25 (20–43)	27.96 ± 5.88 (20–40)	.405	28.85 ± 5.42 (21–38)	26.63 ± 6.82 (20–43)	.107
Clinical characteristics								
Cancer stage, No. (%)								
II	9 (20.00%)	8 (24.24%)	5 (23.81%)	4 (16.67%)	.823	3 (11.11%)	5 (31.25%)	.118
III	36 (80.00%)	25 (75.76%)	16 (76.19%)	20 (83.33%)		24 (88.89%)	11 (46.75%)	
Subtype, No. (%)								
Luminal A	9 (20.00%)	7 (21.21%)	4 (19.05%)	5 (20.83%)	.943	8 (29.63%)	0	<.001*
Luminal B	22 (48.89%)	15 (45.45%)	11 (52.38%)	11 (45.83%)		13 (48.15%)	9 (56.52%)	
HER2-enriched	8 (17.78%)	5 (15.15%)	4 (19.05%)	4 (16.67%)		1 (3.70%)	7 (43.75%)	
Basal like	6 (13.33%)	6 (18.18%)	2 (9.52%)	4 (16.67%)		6 (22.22%)	0	
Chemotherapy regimen, No. (%)								
AC → T	11 (24.44%)	8 (24.24%)	2 (9.52%)	9 (37.50%)	.076	11 (40.74%)	0	<.001*
EC → T	1 (2.22%)	1 (3.03%)	1 (4.76%)	0		0	0	
TAC	15 (33.33%)	12 (36.36%)	10 (47.62%)	5 (20.83%)		15 (55.56%)	0	
AT	1 (2.22%)	1 (3.03%)	1 (4.76%)	0		1 (3.70%)	0	
TC	1 (2.22%)	1 (3.03%)	0	1 (4.17%)		0	0	
TCbHP	11 (24.44%)	6 (18.18%)	4 (19.05%)	7 (29.17%)		0	11 (46.75%)	
TCbHB	5 (11.11%)	4 (12.12%)	3 (14.29%)	2 (8.33%)		0	5 (31.25%)	

Note: values shown are mean ± SD (MIN - MAX) unless noted otherwise. *$p < .05$.

Abbreviations: AC → T, doxorubicin + cyclophosphamide + docetaxel; AT, doxorubicin + docetaxel; BMI, body mass index; EC → T, epirubicin + cyclophosphamide + docetaxel; MAX, maximum; MIN, minimum; SAS, Self-Rating Anxiety Scale; SD, standard deviation; SDS, Self-Rating Depression Scale; TAC, paclitaxel + doxorubicin + cyclophosphamide; TC, docetaxel + cyclophosphamide; TCbHB, docetaxel + carboplatin + trastuzumab + pyrotinib; TCbHP, docetaxel + carboplatin + trastuzumab + pertuzumab.

TABLE 2 Comparison of the neuropsychological test results between TP0 and TP1

Neuropsychological tests	TP0	TP1	*t* value	*p* value
Working memory				
DST forwards	6.84 ± 1.37	7.06 ± 1.32	−1.42	.16
DST backwards	4.55 ± 1.23	4.48 ± 1.15	0.47	.64
Executive function and psychomotor speed				
TMT-A	64.21 ± 35.36	57.48 ± 34.91	1.08	.29
Mental flexibility				
VFT	35.81 ± 8.53	37.97 ± 10.28	−1.68	.10
General cognition				
FACT-Cog total	108.65 ± 14.10	109.55 ± 8.10	−0.32	.75
PCI	58.88 ± 9.75	59.85 ± 5.20	−0.47	.64
OTH	15.13 ± 2.74	15.72 ± 0.68	−1.16	.25
PCA	20.24 ± 4.51	19.30 ± 2.49	0.96	.34
QOL	14.41 ± 2.47	14.69 ± 1.86	−0.63	.53

Note: Data are presented as the mean ± SD for normally distributed continuous data and the median (QR) for nonnormally distributed data.

Abbreviations: DST, the digit span test; FCAT-Cog, functional assessment of cancer therapy-cognitive function; OTH, comments from others; PCA, perceived cognitive abilities; PCI, perceived cognitive impairments; QOL, impact on quality of life; SD, standard deviation; TMT-A, the trail making test parts A; TP0, time point 0; TP1, time point 1; VFT, the verbal fluency test.

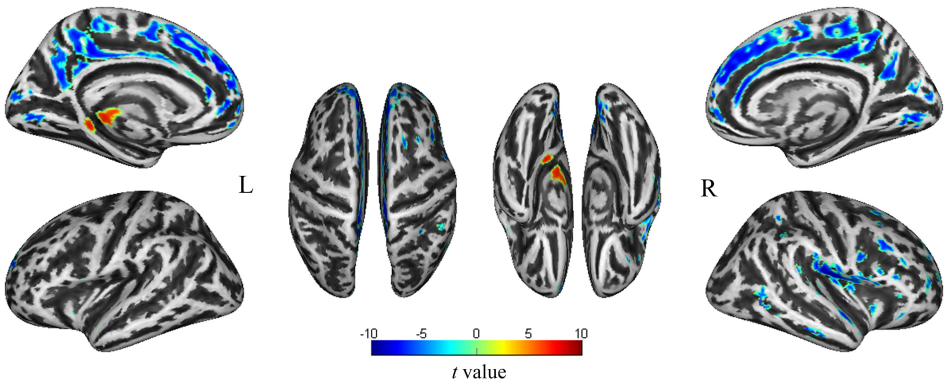

FIGURE 1 Brain regions showing significant changes in GMV after the first cycle of neoadjuvant chemotherapy. The results were corrected by peak-level FWE-corrected $p < .05$ with a cluster extent threshold of 50 voxels. Blue color indicates regions with significant gray matter volume reduction, and red color indicates regions with significant gray matter volume increasement. FWE, familywise error rate; GMV, gray matter volume; L, left; R, right

gyrus, right insula, and bilateral occipital lobes. An SD reduction was found at TP1 in the bilateral frontal lobes, bilateral temporal lobes, bilateral occipital lobes, and left cingulate gyrus compared to TP0, while an SD increment was found in the right insula. GI reductions were found in the bilateral frontal lobes, bilateral parietal lobes, right insula, and right superior temporal gyrus at TP1 compared to TP0. FD reductions were found in the bilateral occipital lobes, left cingulate gyrus and left parahippocampal gyrus, whereas FD increments were found in the bilateral frontal lobes and left postcentral gyrus. The SBM results were corrected by peak-level FWE–corrected $p < .05$ with a cluster extend threshold of 50 voxels/vertexes (Figure 2, Table 4).

More widespread alterations in cortical morphology were found when corrected by peak-level FWE-corrected $p < .05$ without a cluster extend threshold (see Supporting Information, Tables S1, S2 and Figures S1, S2).

In post-hoc analyses, the results of significant differential cortical morphology between subgroups are shown in Tables 5,6. For subgroups divided by age, breast cancer patients in the younger subgroup manifested a larger degree of CT reduction in the right precentral gyrus and superior frontal gyrus comparing with the older subgroup. Breast cancer patients in the older subgroup manifested a larger degree of SD increase in the right insula comparing with the younger subgroup. Among them, the younger subgroup showed a higher CT in the right precentral gyrus at TP0. For subgroups divided by treatment, breast cancer patients showed differential morphological index alterations from TP0 to TP1 between subgroup A and subgroup PB, while no significant differences were found in morphological indices at TP0.

3.4 | Correlation analyses

Brain regions with significant differences in both VBM and at least one SBM index are shown in Table 7. Correlation analyses showed significant correlations between VBM and at least one SBM index in

TABLE 3 Brain regions showing significant changes in GMV

Comparison	Hemisphere	Brain lobe	Brain region	Size (voxels)	MNI coordinate x (mm)	y (mm)	z (mm)	Peak *t* value	Peak-level *p* value (FWE-corrected)
TP1 < TP0	R	Frontal lobe	Superior frontal gyrus, dorsolateral	221	21	66	10.5	−6.42	.003
			Middle frontal gyrus	144	25.5	18	55.5	−6.54	.002
			Inferior frontal gyrus, opercular part	259	46.5	13.5	34.5	−7.36	<.001
		Temporal lobe	Superior temporal gyrus	61	57	−48	21	−5.93	.013
			Middle temporal gyrus	66	61.5	−39	−13.5	−6.38	.003
			Inferior temporal gyrus	145	61.5	−24	−21	−8.11	<.001
		Parietal lobe	Inferior parietal gyrus, excluding supramarginal and angular gyri	64	42	−43.5	52.5	−7.04	<.001
		/	Rolandic operculum	1756	45	−19.5	18	−8.89	<.001
	L	Frontal lobe	Superior frontal gyrus, medial	12,119	−1.5	45	27	−9.56	<.001
			Inferior frontal gyrus, pars orbitalis	107	−48	15	−6	−6.95	.001
		Parietal lobe	Inferior parietal gyrus, excluding supramarginal and angular gyri	66	−34.5	−57	48	−6.01	.010
TP1 > TP0	L	/	Thalamus	320	−15	−31.5	3	7.68	<.001
		Temporal lobe	Hippocampus and parahippocampal	170	−21	−38	−5	7.35	<.001

Note: Corrected for multiple comparisons using the peak-level FWE at a threshold of $p < .05$ with a cluster extend threshold of 50 voxels.
Abbreviations: GMV, gray matter volume; L, left; MNI, montreal neurological institute; R, right; TP0, time point 0; TP1, time point 1.

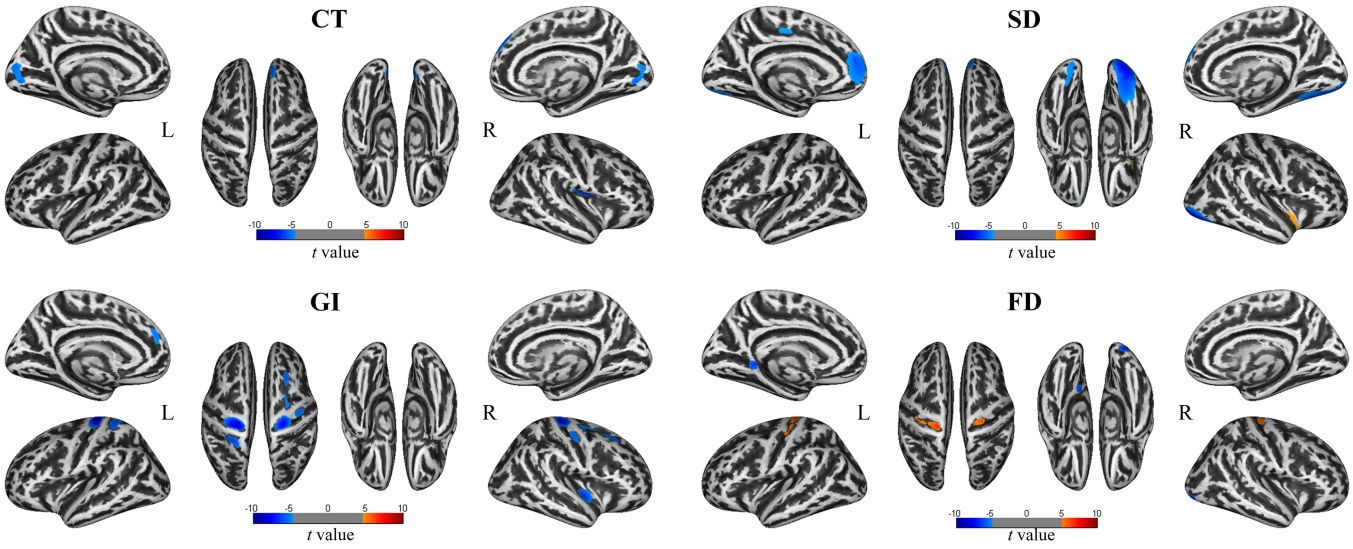

FIGURE 2 Brain regions showing significant changes in CT, SD, GI, and FD after the first cycle of neoadjuvant chemotherapy. The results were corrected by peak-level FWE-corrected $p < .05$ with a cluster extent threshold of 50 vertexes. Blue color indicates regions with significant reduction, and red color indicates regions with significant increasement. CT, cortical thickness; FD, fractal dimension; GI, gyrification index; L, left; R, right; SD, sulcal depth

the bilateral superior frontal gyrus (Figure 3). For clusters with fewer than 50 voxels or vertexes, significant correlations were shown in the left lingual gyrus, right rostral middle frontal gyrus and bilateral post-central gyrus (see Supporting Information, Figure S3).

4 | DISCUSSION

We report the early results of a longitudinal study of cortical morphology alterations in breast cancer patients receiving neoadjuvant

TABLE 4 Brain regions showing significant changes in SBM

Comparison	Hemisphere	Size (vertexes)	Peak *t* value	Peak-level *p* value (FWE-corrected)	Overlap of atlas region	Brain region
Cortical thickness						
TP1 < TP0	R	161	−6.71	<.001	63%	Postcentral gyrus
					25%	Precentral gyrus
					7%	Supramarginal gyrus
					4%	Insula
		113	−5.62	.003	52%	Pericalcarine gyrus
					28%	Lingual gyrus
					19%	Cuneus
		88	−5.68	.003	100%	Superior frontal gyrus
	L	151	−5.61	.003	50%	Pericalcarine gyrus
					28%	Cuneus
					21%	Lingual gyrus
Sulcal depth						
TP1 < TP0	R	710	−7.74	<.001	45%	Lateral occipital gyrus
					41%	Fusiform gyrus
					13%	Lingual gyrus
		98	−5.25	.005	100%	Superior frontal gyrus
	L	322	−6.02	<.001	80%	Superior frontal gyrus
					11%	Rostral anterior cingulate gyrus
					9%	Medial orbitofrontal gyrus
		132	−4.94	.011	55%	Lateral occipital gyrus
					31%	Lingual gyrus
					14%	Fusiform gyrus
		56	−4.62	.028	50%	Paracentral gyrus
					50%	Posterior cingulate gyrus
TP1 > TP0	R	95	4.71	.022	98%	Insula
Gyrification index						
TP1 < TP0	R	271	−7.56	<.001	71%	Precentral gyrus
					29%	Postcentral gyrus
		176	−6.36	<.001	57%	Insula
					43%	Superior temporal gyrus
		117	−5.39	.006	100%	Precentral gyrus
		67	−5.7	.002	52%	Superior frontal gyrus
					48%	Caudal middle frontal gyrus
		62	−4.96	.022	73%	Precentral gyrus
					27%	Superior frontal gyrus
	L	350	−8.35	<.001	71%	Precentral gyrus
					29%	Postcentral gyrus
		162	−6.14	.001	79%	Superior parietal gyrus
					21%	Postcentral gyrus
		59	−5.17	.012	100%	Superior frontal gyrus
Fractal dimension						
TP1 < TP0	R	62	−7.04	<.001	100%	Lateral occipital gyrus
	L	75	−6.20	.001	63%	Isthmus cingulate gyrus
					23%	Lingual gyrus
					13%	Parahippocampal gyrus

TABLE 4 (Continued)

Comparison	Hemisphere	Size (vertexes)	Peak *t* value	Peak-level *p* value (FWE-corrected)	Overlap of atlas region	Brain region
TP1 > TP0	R	87	5.89	.003	100%	Precentral gyrus
	L	107	6.91	<.001	79%	Precentral gyrus
					21%	Postcentral gyrus
		66	5.23	.020	55%	Precentral gyrus
					45%	Postcentral gyrus

Note: Corrected for multiple comparisons using the peak-level FWE at a threshold of $p < .05$ with a cluster extend threshold of 50 vertexes.
Abbreviations: L, left; SBM, surface-based morphometry; R, right; TP0, time point 0; TP1, time point 1.

chemotherapy. The results showed that VBM and SBM indices changed after the first cycle of neoadjuvant chemotherapy. Reductions in GMV, CT, SD, and GI were found in most brain areas, while increments were found to be mainly concentrated in and around the hippocampus. FD was reduced mainly in the limbic and occipital lobes and increased mainly in the anterior and posterior central gyrus. In addition, significant correlations between VBM and at least one SBM index were shown in the bilateral superior frontal gyrus. Altered brain regions in the short term after chemotherapy were found in this study, and their association with cognitive domains will be discussed.

4.1 | Cortical morphology changes related to memory

Memory impairment has been observed in breast cancer patients after chemotherapy (Lange et al., 2019). As reported, memory is mediated primarily by a neural circuit composed of the hippocampus, parahippocampal cortex, thalamus, fornix, mammillary bodies, cingulate gyrus and prefrontal cortex (LaBar & Cabeza, 2006; Vertes et al., 2001; Xu & Südhof, 2013). This circuit, called the Papez circuit after the neuroanatomist who defined it, provides an anatomic substrate for memory maintenance (Aggleton & Brown, 1999). Lesions in each of the major components of the circuit have been shown to disrupt memory (Bueno et al., 2021; Porto et al., 2019).

Our study found cortical morphology alterations in the major components of the Papez circuit. First, GMV was found to be increased in the left hippocampus, parahippocampal gyrus, and thalamus, among which the left parahippocampal gyrus was also found to have increases in FD. Previous studies on breast cancer patients have reported that the hippocampus showed higher connectivity with the left cuneus cortex during a memory task 18 months after chemotherapy (Apple et al., 2018), and hyporesponsiveness of the parahippocampal gyrus was correlated with low performance of episodic memory 10 years after chemotherapy (de Ruiter et al., 2011). Second, we found reductions in SD and FD in the left cingulate gyrus. Similarly, previous studies on breast cancer patients have reported that the bilateral posterior cingulate gyrus exhibited impaired white matter integrity and decreased metabolic activity along with memory loss 2 or 3 weeks after chemotherapy completion(Tong et al., 2020). Finally, we found a large area of GMV reduction in the prefrontal lobes, mainly concentrated on the medial side. GMV showed a positive correlation with CT, SD, GI, and FD in the right superior frontal gyrus and with SD in the left superior frontal gyrus. A previous longitudinal study showed decreased functional activation in the frontal gyrus with a high-working memory load 1 month after breast cancer chemotherapy completion, which returned to normal 1 year later(McDonald et al., 2012). And lower gray matter density in the right middle frontal gyrus 1 month after chemotherapy completion was positively correlated with disrupted memory retrieval (Li et al., 2018).

4.2 | Cortical morphology changes related to executive function

Executive function reduction has been observed in breast cancer patients after chemotherapy (Ganz et al., 2013). Controlled by the central executive network (CEN), executive function is responsible for a set of higher-order cognitive functions, including working memory, inhibition, and task switching (Diamond, 2013). CEN is mainly distributed in the prefrontal lobes, anterior cingulate cortex, inferior parietal lobule (Vincent et al., 2008), and most areas of the middle temporal gyrus and posterior inferior temporal gyrus (O'Neill et al., 2019).

Our study found cortical morphology alterations in the major components of the CEN. On the one hand, we found a reduction in GMV in a large area of the prefrontal lobes that was mainly concentrated on the medial side. A partial area of the prefrontal lobes showed a reduction in CT, SD, and GI, and an increase in FD. Previous studies on breast cancer patients have reported that a reduction in GMV in the frontal lobes was positively related to poorer performance on executive function after chemotherapy (Lepage et al., 2014). Gray matter density reduction in the bilateral middle frontal gyrus was found to be correlated with executive dysfunction 1 month after chemotherapy completion (Li et al., 2018; McDonald et al., 2013b). On the other hand, we found that the left rostral anterior cingulate showed a decrease in SD. Previous studies showed that, several years after chemotherapy, reduced activation and functional connectivity in the CEN correlated with elevated executive

TABLE 5 Brain regions showing significant changes in subgroups divided by age

Morphometry indices	Brain regions	TP1 − TP0			TP0		
		Younger subgroup $n = 21$	Older subgroup $n = 24$	p value	Younger subgroup $n = 21$	Older subgroup $n = 24$	p value
CT (mm)	Right precentral gyrus	−0.041 (−0.097, 0.032)	0.060 (−0.006, 0.110)	0.019*	2.541 (2.468, 2.600)	2.437 (2.350, 2.539)	.042*
	Right superior frontal gyrus	−0.015 (−0.025, 0.017)	0.012 (−0.011, 0.050)	0.022*	2.812 (2.780, 2.865)	2.795 (2.736, 2.923)	.609
SD (mm)	Right insula	−0.016 (−0.076, 0.076)	0.096 (−0.010, 0.149)	0.015*	24.216 ± 0.300	23.636 ± 0.236	.132

Note: *$p < .05$. Mean ± SD or median (IQR) were used according to the distribution of data.
Abbreviations: CT, cortical thickness; SD, sulcal depth; TP0, time point 0; TP1, time point 1.

TABLE 6 Brain regions showing significant changes in subgroups divided by treatment

Morphometry indices	Brain regions	TP1 − TP0			TP0		
		Subgroup A $n = 18$	Subgroup PB $n = 27$	p value	Subgroup A $n = 18$	Subgroup PB $n = 27$	p value
GMV (cm^3)	Left superior frontal gyrus, medial	−0.010 (−0.015, −0.007)	−0.003 (−0.015, 0.004)	.035*	0.341 (0.317, 0.359)	0.338 (0.313, 0.374)	.960
	Right superior frontal gyrus, dorsolateral	−0.005 (−0.007, −0.002)	0.000 (−0.007, 0.006)	.031*	0.287 ± 0.033	0.288 ± 0.032	.953
	Left thalamus	−0.004 (−0.009, 0.031)	0.037 (0.005, 0.049)	.013*	0.389 ± 0.039	0.393 ± 0.051	.768
CT (mm)	Left lingual gyrus	0.012 ± 0.044	−0.023 ± 0.061	.037*	1.942 (1.893, 2.010)	1.941 (1.877, 2.040)	.651
SD (mm)	Right insula	−0.016 (−0.081, 0.097)	0.075 (0.000,0.152)	.042*	23.738 ± 1.302	24.258 ± 1.286	.210
FD	Left postcentral gyrus	−0.001 ± 0.008	0.004 ± 0.007	.041*	2.821 ± 0.100	2.802 ± 0.127	.593

Note: *$p < .05$. Mean ± SD or median (IQR) were used according to the distribution of data.
Abbreviations: DST, the digit span test; FCAT-Cog, functional assessment of cancer therapy-cognitive function; OTH, comments from others; PCA, perceived cognitive abilities; PCI, perceived cognitive impairments; QOL, impact on quality of life; SD, standard deviation; TMT-A, the trail making test parts A; TP0, time point 0; TP1, time point 1; VFT, the verbal fluency test.

dysfunction, especially in the prefrontal lobes and anterior cingulate gyrus (de Ruiter et al., 2011; Kesler et al., 2011; Miao, Li, et al., 2016; Wang et al., 2016).

TABLE 7 Altered brain regions showing overlaps of VBM and SBM

Brain region	GMV	CT	SD	GI	FD
R caudal middle frontal gyrus	↓			↓	
R lateral occipital gyrus			↓		↓
L lingual gyrus		↓	↓		↓
R lingual gyrus		↓	↓		
L parahippocampal gyrus	↑				↓
L postcentral gyrus				↓	↑
R postcentral gyrus		↓		↓	
L precentral gyrus				↓	↑
R precentral gyrus		↓		↓	↑
R rostral middle frontal gyrus	↓				↑
L superior frontal gyrus	↓		↓	↓	
R superior frontal gyrus	↓	↓	↓	↓	↑
R superior temporal gyrus	↓			↓	
R insula		↓	↑	↓	

Note: The above ↓ means reduction and ↑ means increment after chemotherapy.
Abbreviations: CT, cortical thickness; FD, fractal dimension; GI, gyrification index; GMV, gray matter volume; L, left; R, right; SBM, surface-based morphometry; SD, sulcal depth; VBM, voxel-based morphometry.

4.3 | Cortical morphology changes related to attention and processing speed

Dysfunction in attention and processing speed has been observed in breast cancer patients after chemotherapy (Wefel et al., 2015). Attention networks in the human brain are separated into dorsal and ventral systems (Corbetta & Shulman, 2002). The dorsal attention network (DAN) derives from the frontoparietal lobes and reacts at the occipital lobes. The ventral attention network comprises the temporoparietal junction and the ventral frontal cortex (Vossel et al., 2014). Similarly, closely related to the concentration of attention, information processing speed depends upon the parietal and temporal lobes and middle frontal gyrus (Turken et al., 2008).

Our study found cortical morphology alterations in the major components of the attention and processing speed system. First, we found a large area of decreased GMV in the frontal, parietal and temporal lobes. Previous neuroimaging studies also reported that structural and functional alterations in the brain after chemotherapy were correlated with attention and processing speed (Lange et al., 2019). In structural studies, GMV loss in the frontal, temporal, and occipital areas in breast cancer patients had a positive relationship with processing speed 1 month after chemotherapy completion (Lepage et al., 2014). Performance on neuropsychological tests of attention and processing speed correlated significantly with the integrity of frontal, parietal, temporal and occipital white matter tracts after chemotherapy (Deprez et al., 2011; Deprez et al., 2012). In fMRI studies, changes in DAN-associated brain regions were also reported after breast cancer chemotherapy (Miao, Chen, et al., 2016; Shen

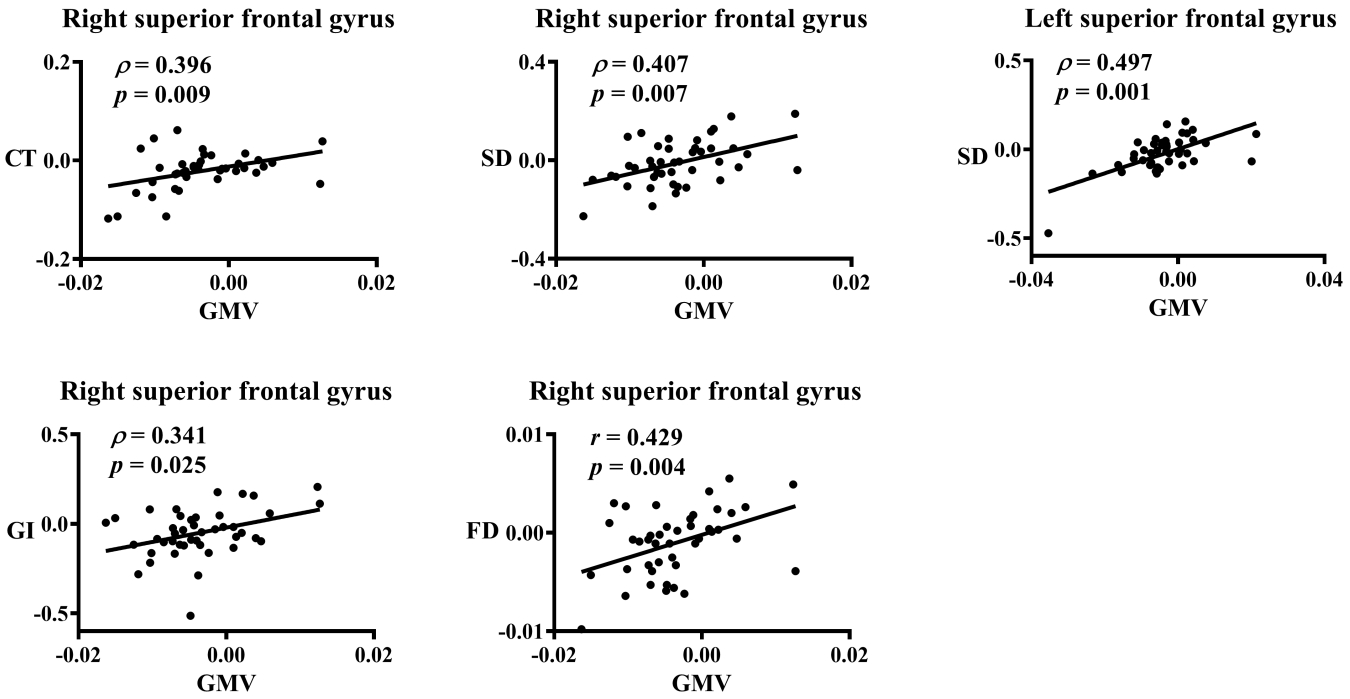

FIGURE 3 Correlations between the longitudinal changes in the VBM data and those in the four indices of SBM data in the same brain regions. Longitudinal changes calculated as extracted image value at TP1 minus that at TP0. ρ = Spearman's rank correlation coefficient; r = Pearson correlation coefficient. CT, cortical thickness; FD, fractal dimension; GI, gyrification index; L, left; R, right; SD, sulcal depth

et al., 2019). Using arterial spin labeling perfusion, one study showed significant increases in cerebral blood flow in breast cancer patients 1 month after chemotherapy that were associated with altered attention networks(Chen et al., 2017). Second, the SBM results showed varying degrees of reduction in CT, SD, and GI in the frontal, parietal, temporal and occipital lobes. FD alterations were more complex in the mentioned lobes. Specifically, the frontal and parietal lobes showed an increase, and the occipital lobes showed a decrease. GMV showed a positive correlation with CT in the left lingual gyrus (Supporting Information, Figure S3). Changes in SBM indices have been reported in many studies of psychiatric disorders (Matsuda & Ohi, 2018; Wolf et al., 2021) and neurodegeneration (Huang et al., 2021; Im et al., 2008), but their impacts on cognition in breast cancer patients undergoing chemotherapy have not yet been reported. This study may suggest that the effect of chemotherapy on the cortical structure of breast cancer patients is reflected in both altered GMV and a series of comprehensive changes in morphological indices.

4.4 | Cortical morphology changes in the insula

Our study also found changes in the insula, which have rarely been covered by other studies about chemotherapy-related cognitive impairment in breast cancer patients. In our study, we found that the right insula showed an increase in SD and a decrease in GMV and GI. The bilateral insula showed a decrease in CT (Supporting Information, Tables S1–S3). In a VBM study, gray matter density reduction was found in the right insula from baseline to 1 month after postoperative chemotherapy completion in breast cancer patients (Chen et al., 2018). As a component of the salience network (Seeley et al., 2007), the insula can integrate external sensory information with internal emotional and bodily state signals to coordinate brain network dynamics and to initiate switches between the default mode network and CEN (Uddin, 2015). In tasks requiring greater cognitive control, the dorsal anterior insula exerts a stronger causal influence (Cai et al., 2016). Currently, studies on insular cortex function are not limited to the initial features of the limbic cortex, including sensorimotor, pain, and social–emotional processes, but focus more on high-level attention and decision-making (Uddin et al., 2017). Our study suggests that changes in the insula cannot be ignored in future studies on chemotherapy-related cognitive impairment in breast cancer patients.

4.5 | Cortical morphology changes in subgroups divided by age and treatment

Cortical morphology changed with normal structural brain aging in previous studies (Zhao et al., 2019). Whether the original cortical morphology of different age influence the subsequent alteration by chemotherapy is unclear. Our exploratory study found that longitudinal differences of CT and SD were existed in some brain regions between the younger subgroup and the older subgroup. Interestingly, breast cancer patients in younger subgroup which has higher morphologic indices (significant difference or potential tendency) showed more likely to decline in brain regions that decreased after neoadjuvant chemotherapy. This finding suggested that breast cancer patients show different susceptibilities to chemotherapy, which may be related to the different cortical morphometry caused by age itself.

Previous studies showed that anthracyclines may have negative effects on brain network connections (Kesler & Blayney, 2016) and white matter integrity (Menning et al., 2018). In this study, under the circumstance of no significant differences in morphological indices at TP0, breast cancer patients showed differential morphological index alterations from TP0 to TP1 between subgroup A and subgroup PB. In line with previous studies, breast cancer patients who received anthracyclines were more likely to show declines in morphological indices. This result suggested that therapeutic regimen may affect cortical morphology remodeling after chemotherapy.

4.6 | Cognitive functions

We found no significant differences in the cognition-related neuropsychological test results before and after chemotherapy, while the altered brain regions were in line with those associated with impaired cognitive domains in previous studies. First, these results were indicative of the fact that chemotherapy-related cognitive impairment is often subclinical and with great interindividual differences. In addition, the interval of the neuropsychological tests at TP0 and TP1 might have been too short to observe the cognitive impact of chemotherapy. Neuropsychological tests might not be sufficiently sensitive to detect subtle changes. In addition, the lack of neuropsychological tests in 12 of 45 participants might be an explanatory factor. Finally, it cannot be ruled out that the alterations of those cortical morphologies were caused by inflammatory edema or decreased tissue water content under the cytotoxicity of chemotherapeutic drugs (Pomares et al., 2017).

A positive trend of cognitive status was shown in most tests after chemotherapy. There are three possible explanations. First, due to the short interval and single stimulation, subtle intrasubject cognitive differences may not have been obtained from neuropsychological tests. Moreover, due to the practice effect, the short-term interval of approximately 1 month may have made patients more familiar with the tests. Finally, patients' emotional shock at the time of initial diagnosis may have been alleviated after embarking on a regular treatment regimen.

The advantages of this study are as follows. Our study was a longitudinal study and observed the early response to chemotherapy in breast cancer patients, showing the changes in cortical morphology from a comprehensive perspective, including VBM and SBM. Meanwhile, patients receiving neoadjuvant chemotherapy were recruited to eliminate the interference of anesthesia in surgery. This may indicate major changes in early brain damage after chemotherapy and before cognitive impairment arises. What's more, results of post-hoc analyses in subgroups divided by age and treatment may provide a possibility for better understanding chemotherapy related cognitive impairment.

Limitations of this study should be mentioned. First, 12 subjects failed to properly complete the psychological tests because of noncooperation. Future studies should try to avoid this situation by enlarging the sample size and removing residual values. Second, no differences were found in the psychological test results between TP0 and TP1. More cognitive tests will be selected to comprehensively cover the cognitive domains in future studies. Third, in this study, patients receiving hormone therapy were excluded, but the interference of estrogen changes in vivo was not excluded. In the Supporting Information, compared to breast cancer patients before menopause, those after menopause showed a more significant increase in GMV in the left thalamus. Further studies should be carried out to explore the relationship of estrogen status in breast cancer patients and the structure and function of the thalamus after chemotherapy. In addition, the chemotherapy regimens in our study included classical chemotherapy and chemotherapy with targeted therapy. Due to small samples in such subgroups, studies of larger populations are needed in the future. Finally, our study lacked a breast cancer control group who did not receive chemotherapy and a healthy control group. According to previous studies and considering the short-term setting in this longitudinal study, we believe that the aging effects on cortical morphology in such control groups can be ignored (Deprez et al., 2011; McDonald et al., 2013b). The lack of control groups makes it difficult to interpret whether potential changes could have arisen by learning effects in the psychological tests or status of anxiety and depression. If long-term follow-up is needed in the future, it would be better to include control groups with data acquisition time intervals the same as those of breast cancer patients who received chemotherapy.

5 | CONCLUSION

We report the early results of a longitudinal study of cortical morphology alterations in breast cancer patients receiving neoadjuvant chemotherapy. The results showed no significant changes in neuropsychological test results, while both VBM and SBM indices changed after the first cycle of neoadjuvant chemotherapy. The affected brain regions are consistent with those associated with impaired cognitive domains in previous studies. These findings may indicate major targets of early brain damage after chemotherapy.

ACKNOWLEDGMENTS

This work was supported by the National Natural Science Foundation of China (No. 82071883), Graduate Research and Innovation Foundation of Chongqing, China (No. CYS21071), Chongqing Natural Science Foundation (Nos. cstc2021jcyj-msxmX0319 and cstc2021jcyj-msxmX0313), Chongqing Medical Research Project of Combination of Science and Medicine (No. 2021MSXM035), and 2020 SKY Imaging Research Fund of the Chinese International Medical Foundation (No. Z-2014-07-2003-24).

FUNDING INFORMATION

National Natural Science Foundation of China, Grant/Award Number: 82071883; Graduate Research and Innovation Foundation of Chongqing, China, Grant/Award Number: CYS21071; Chongqing Natural Science Foundation, Grant/Award Number: cstc2021jcyj-msxmX0319; cstc2021jcyj-msxmX0313; Chongqing Medical Research Project of Combination of Science and Medicine, Grant/Award Number: 2021MSXM035; 2020 SKY Imaging Research Fund of the Chinese International Medical Foundation, Grant/Award Number: Z-2014-07-2003-24.

CONFLICT OF INTERESTS

The authors declare no conflict of interests.

DATA AVAILABILITY STATEMENT

The data in this manuscript are a part of a longitudinal study that will generate more than one manuscript. The data will be available upon completion of these manuscripts. Original data can be made available upon reasonable request.

ORCID

Jiuquan Zhang https://orcid.org/0000-0003-0239-6988

REFERENCES

Aggleton, J. P., & Brown, M. W. (1999). Episodic memory, amnesia, and the hippocampal-anterior thalamic axis. *The Behavioral and Brain Sciences*, *22*, 425–444.

Apple, A. C., Schroeder, M. P., Ryals, A. J., Wagner, L. I., Cella, D., Shih, P. A., Reilly, J., Penedo, F. J., Voss, J. L., & Wang, L. (2018). Hippocampal functional connectivity is related to self-reported cognitive concerns in breast cancer patients undergoing adjuvant therapy. *Neuroimage Clinical*, *20*, 110–118. https://doi.org/10.1016/j.nicl.2018.07.010

Billiet, T., Emsell, L., Vandenbulcke, M., Peeters, R., Christiaens, D., Leemans, A., van Hecke, W., Smeets, A., Amant, F., Sunaert, S., & Deprez, S. (2018). Recovery from chemotherapy-induced white matter changes in young breast cancer survivors? *Brain Imaging and Behavior*, *12*, 64–77. https://doi.org/10.1007/s11682-016-9665-8

Bowie, C. R., & Harvey, P. D. (2006). Administration and interpretation of the trail making test. *Nature Protocols*, *1*, 2277–2281. https://doi.org/10.1038/nprot.2006.390

Bueno, A. P. A., de Souza, L. C., Pinaya, W. H. L., Teixeira, A. L., de Prado, L. G. R., Caramelli, P., Hornberger, M., & Sato, J. R. (2021). Papez circuit gray matter and episodic memory in amyotrophic lateral sclerosis and behavioural variant frontotemporal dementia. *Brain Imaging and Behavior*, *15*, 996–1006. https://doi.org/10.1007/s11682-020-00307-5

Cai, W., Chen, T., Ryali, S., Kochalka, J., Li, C. S. R., & Menon, V. (2016). Causal interactions within a frontal-cingulate-parietal network during cognitive control: Convergent evidence from a multisite-multitask investigation. *Cerebral Cortex*, *26*, 2140–2153. https://doi.org/10.1093/cercor/bhv046

Chen, B. T., Jin, T., Patel, S. K., Ye, N., Sun, C. L., Ma, H., Rockne, R. C., Root, J. C., Saykin, A. J., Ahles, T. A., Holodny, A. I., Prakash, N., Mortimer, J., Waisman, J., Yuan, Y., Li, D., Somlo, G., Vazquez, J., Levi, A., … Hurria, A. (2018). Gray matter density reduction associated with adjuvant chemotherapy in older women with breast cancer. *Breast Cancer Research and Treatment*, *172*, 363–370. https://doi.org/10.1007/s10549-018-4911-y

Chen, X., He, X., Tao, L., Cheng, H., Li, J., Zhang, J., Qiu, B., Yu, Y., & Wang, K. (2017). The attention network changes in breast cancer patients receiving neoadjuvant chemotherapy: Evidence from an arterial spin labeling perfusion study. *Scientific Reports*, *7*, 42684. https://doi.org/10.1038/srep42684

Clarkson, M. J., Cardoso, M. J., Ridgway, G. R., Modat, M., Leung, K. K., Rohrer, J. D., Fox, N. C., & Ourselin, S. (2011). A comparison of voxel and surface based cortical thickness estimation methods. *NeuroImage*, *57*, 856–865. https://doi.org/10.1016/j.neuroimage.2011.05.053

Corbetta, M., & Shulman, G. L. (2002). Control of goal-directed and stimulus-driven attention in the brain. *Nature Reviews. Neuroscience*, *3*, 201–215. https://doi.org/10.1038/nrn755

Damme, K. S. F., Gupta, T., Nusslock, R., Bernard, J. A., Orr, J. M., & Mittal, V. A. (2019). Cortical morphometry in the psychosis risk period: A comprehensive perspective of surface features. *Biological Psychiatry Cognitive Neuroscience and Neuroimaging*, *4*, 434–443. https://doi.org/10.1016/j.bpsc.2018.01.003

de Ruiter, M. B., Reneman, L., Boogerd, W., Veltman, D. J., Caan, M., Douaud, G., Lavini, C., Linn, S. C., Boven, E., van Dam, F. S. A. M., & Schagen, S. B. (2012). Late effects of high-dose adjuvant chemotherapy on white and gray matter in breast cancer survivors: Converging results from multimodal magnetic resonance imaging. *Human Brain Mapping*, *33*, 2971–2983. https://doi.org/10.1002/hbm.21422

de Ruiter, M. B., Reneman, L., Boogerd, W., Veltman, D. J., van Dam, F. S. A. M., Nederveen, A. J., Boven, E., & Schagen, S. B. (2011). Cerebral hyporesponsiveness and cognitive impairment 10 years after chemotherapy for breast cancer. *Human Brain Mapping*, *32*, 1206–1219. https://doi.org/10.1002/hbm.21102

Deprez, S., Amant, F., Smeets, A., Peeters, R., Leemans, A., van Hecke, W., Verhoeven, J. S., Christiaens, M. R., Vandenberghe, J., Vandenbulcke, M., & Sunaert, S. (2012). Longitudinal assessment of chemotherapy-induced structural changes in cerebral white matter and its correlation with impaired cognitive functioning. *Journal of Clinical Oncology*, *30*, 274–281. https://doi.org/10.1200/jco.2011.36.8571

Deprez, S., Amant, F., Yigit, R., Porke, K., Verhoeven, J., Stock, J. V., Smeets, A., Christiaens, M. R., Leemans, A., Hecke, W. V., Vandenberghe, J., Vandenbulcke, M., & Sunaert, S. (2011). Chemotherapy-induced structural changes in cerebral white matter and its correlation with impaired cognitive functioning in breast cancer patients. *Human Brain Mapping*, *32*, 480–493. https://doi.org/10.1002/hbm.21033

Diamond, A. (2013). Executive functions. *Annual Review of Psychology*, *64*, 135–168. https://doi.org/10.1146/annurev-psych-113011-143750

Fischl, B., & Dale, A. M. (2000). Measuring the thickness of the human cerebral cortex from magnetic resonance images. *Proceedings of the National Academy of Sciences of the United States of America*, *97*, 11050–11055. https://doi.org/10.1073/pnas.200033797

Ganz, P. A., Kwan, L., Castellon, S. A., Oppenheim, A., Bower, J. E., Silverman, D. H. S., Cole, S. W., Irwin, M. R., Ancoli-Israel, S., & Belin, T. R. (2013). Cognitive complaints after breast cancer treatments: Examining the relationship with neuropsychological test performance. *Journal of the National Cancer Institute*, *105*, 791–801. https://doi.org/10.1093/jnci/djt073

Henry, J. D., Crawford, J. R., & Phillips, L. H. (2004). Verbal fluency performance in dementia of the Alzheimer's type: A meta-analysis. *Neuropsychologia*, *42*, 1212–1222. https://doi.org/10.1016/j.neuropsychologia.2004.02.001

Hirayama, S., Terasawa, K., Rabeler, R., Hirayama, T., Inoue, T., Tatsumi, Y., Purpura, M., & Jäger, R. (2014). The effect of phosphatidylserine administration on memory and symptoms of attention-deficit hyperactivity disorder: A randomised, double-blind, placebo-controlled clinical trial. *Journal of Human Nutrition and Dietetics*, *27*(Suppl 2), 284–291. https://doi.org/10.1111/jhn.12090

Huang, K. L., Hsiao, I. T., Chang, T. Y., Yang, S. Y., Chang, Y. J., Wu, H. C., Liu, C. H., Wu, Y. M., Lin, K. J., Ho, M. Y., & Lee, T. H. (2021). Neurodegeneration and vascular burden on cognition after midlife: A plasma and neuroimaging biomarker study. *Frontiers in Human Neuroscience*, *15*, 735063. https://doi.org/10.3389/fnhum.2021.735063

Im, K., Lee, J. M., Seo, S. W., Hyumg Kim, S., Kim, S. I., & Na, D. L. (2008). Sulcal morphology changes and their relationship with cortical thickness and gyral white matter volume in mild cognitive impairment and Alzheimer's disease. *NeuroImage*, *43*, 103–113. https://doi.org/10.1016/j.neuroimage.2008.07.016

Im, K., Lee, J. M., Yoon, U., Shin, Y. W., Hong, S. B., Kim, I. Y., Kwon, J. S., & Kim, S. I. (2006). Fractal dimension in human cortical surface: Multiple regression analysis with cortical thickness, sulcal depth, and folding area. *Human Brain Mapping*, *27*, 994–1003. https://doi.org/10.1002/hbm.20238

Inagaki, M., Yoshikawa, E., Matsuoka, Y., Sugawara, Y., Nakano, T., Akechi, T., Wada, N., Imoto, S., Murakami, K., Uchitomi, Y., & The Breast Cancer Survivors' Brain MRI Database Group. (2007). Smaller regional volumes of brain gray and white matter demonstrated in breast cancer survivors exposed to adjuvant chemotherapy. *Cancer*, *109*, 146–156. https://doi.org/10.1002/cncr.22368

Janelsins, M. C., Heckler, C. E., Peppone, L. J., Kamen, C., Mustian, K. M., Mohile, S. G., Magnuson, A., Kleckner, I. R., Guido, J. J., Young, K. L., Conlin, A. K., Weiselberg, L. R., Mitchell, J. W., Ambrosone, C. A., Ahles, T. A., & Morrow, G. R. (2017). Cognitive complaints in survivors of breast cancer after chemotherapy compared with age-matched controls: An analysis from a nationwide, multicenter, prospective longitudinal study. *Journal of Clinical Oncology*, *35*, 506–514. https://doi.org/10.1200/JCO.2016.68.5826

Kesler, S. R., & Blayney, D. W. (2016). Neurotoxic effects of Anthracycline- vs. nonanthracycline-based chemotherapy on cognition in breast cancer survivors. *JAMA Oncology*, *2*, 185–192. https://doi.org/10.1001/jamaoncol.2015.4333

Kesler, S. R., Kent, J. S., & O'Hara, R. (2011). Prefrontal cortex and executive function impairments in primary breast cancer. *Archives of Neurology*, *68*, 1447–1453. https://doi.org/10.1001/archneurol.2011.245

Koppelmans, V., de Ruiter, M. B., van der Lijn, F., Boogerd, W., Seynaeve, C., van der Lugt, A., Vrooman, H., Niessen, W. J., Breteler, M. M. B., & Schagen, S. B. (2012). Global and focal brain volume in long-term breast cancer survivors exposed to adjuvant chemotherapy. *Breast Cancer Research and Treatment*, *132*, 1099–1106. https://doi.org/10.1007/s10549-011-1888-1

LaBar, K. S., & Cabeza, R. (2006). Cognitive neuroscience of emotional memory. *Nature Reviews. Neuroscience*, *7*, 54–64. https://doi.org/10.1038/nrn1825

Lamballais, S., Vinke, E. J., Vernooij, M. W., Ikram, M. A., & Muetzel, R. L. (2020). Cortical gyrification in relation to age and cognition in older adults. *NeuroImage*, *212*, 116637. https://doi.org/10.1016/j.neuroimage.2020.116637

Lange, M., Joly, F., Vardy, J., Ahles, T., Dubois, M., Tron, L., Winocur, G., de Ruiter, M. B., & Castel, H. (2019). Cancer-related cognitive impairment: An update on state of the art, detection, and management strategies in cancer survivors. *Annals of Oncology*, *30*, 1925–1940. https://doi.org/10.1093/annonc/mdz410

Lepage, C., Smith, A. M., Moreau, J., Barlow-Krelina, E., Wallis, N., Collins, B., MacKenzie, J., & Scherling, C. (2014). A prospective study of grey matter and cognitive function alterations in chemotherapy-treated breast cancer patients. *Springerplus*, *3*, 444. https://doi.org/10.1186/2193-1801-3-444

Li, X., Chen, H., Lv, Y., Chao, H. H., Gong, L., Li, C. S. R., & Cheng, H. (2018). Diminished gray matter density mediates chemotherapy dosage-related cognitive impairment in breast cancer patients. *Scientific Reports*, *8*, 13801. https://doi.org/10.1038/s41598-018-32257-w

Luders, E., Thompson, P. M., Narr, K. L., Toga, A. W., Jancke, L., & Gaser, C. (2006). A curvature-based approach to estimate local gyrification on the cortical surface. *NeuroImage*, *29*, 1224–1230. https://doi.org/10.1016/j.neuroimage.2005.08.049

Matsos, A., Loomes, M., Zhou, I., Macmillan, E., Sabel, I., Rotziokos, E., Beckwith, W., & Johnston, I. N. (2017). Chemotherapy-induced cognitive impairments: White matter pathologies. *Cancer Treatment Reviews*, *61*, 6–14. https://doi.org/10.1016/j.ctrv.2017.09.010

Matsuda, Y., & Ohi, K. (2018). Cortical gyrification in schizophrenia: Current perspectives. *Neuropsychiatric Disease and Treatment*, *14*, 1861–1869. https://doi.org/10.2147/ndt.S145273

McDonald, B. C., Conroy, S. K., Ahles, T. A., West, J. D., & Saykin, A. J. (2010). Gray matter reduction associated with systemic chemotherapy for breast cancer: A prospective MRI study. *Breast Cancer Research and Treatment*, *123*, 819–828. https://doi.org/10.1007/s10549-010-1088-4

McDonald, B. C., Conroy, S. K., Ahles, T. A., West, J. D., & Saykin, A. J. (2012). Alterations in brain activation during working memory processing associated with breast cancer and treatment: A prospective functional magnetic resonance imaging study. *Journal of Clinical Oncology*, *30*, 2500–2508. https://doi.org/10.1200/jco.2011.38.5674

McDonald, B. C., Conroy, S. K., Smith, D. J., West, J. D., & Saykin, A. J. (2013a). Frontal gray matter reduction after breast cancer chemotherapy and association with executive symptoms: A replication and extension study. *Brain, Behavior, and Immunity*, *30*, S117–S125. https://doi.org/10.1016/j.bbi.2012.05.007

McDonald, B. C., Conroy, S. K., Smith, D. J., West, J. D., & Saykin, A. J. (2013b). Frontal gray matter reduction after breast cancer chemotherapy and association with executive symptoms: A replication and extension study. *Brain, Behavior, and Immunity*, *30*, S117–S125. https://doi.org/10.1016/j.bbi.2012.05.007

Menning, S., de Ruiter, M. B., Veltman, D. J., Boogerd, W., Oldenburg, H. S. A., Reneman, L., & Schagen, S. B. (2018). Changes in brain white matter integrity after systemic treatment for breast cancer: A prospective longitudinal study. *Brain Imaging and Behavior*, *12*, 324–334. https://doi.org/10.1007/s11682-017-9695-x

Miao, H., Chen, X., Yan, Y., He, X., Hu, S., Kong, J., Wu, M., Wei, Y., Zhou, Y., Wang, L., Wang, K., & Qiu, B. (2016). Functional connectivity change of brain default mode network in breast cancer patients after chemotherapy. *Neuroradiology*, *58*, 921–928. https://doi.org/10.1007/s00234-016-1708-8

Miao, H., Li, J., Hu, S., He, X., Partridge, S. C., Ren, J., Bian, Y., Yu, Y., & Qiu, B. (2016). Long-term cognitive impairment of breast cancer patients after chemotherapy: A functional MRI study. *European Journal of Radiology*, *85*, 1053–1057. https://doi.org/10.1016/j.ejrad.2016.03.011

Mustafa, N., Ahearn, T. S., Waiter, G. D., Murray, A. D., Whalley, L. J., & Staff, R. T. (2012). Brain structural complexity and life course cognitive change. *NeuroImage*, *61*, 694–701. https://doi.org/10.1016/j.neuroimage.2012.03.088

Niu, R., Du, M., Ren, J., Qing H., Wang, X., Xu, G., Lei, D., & Zhou, P. (2021). Chemotherapy-induced grey matter abnormalities in cancer survivors: A voxel-wise neuroimaging meta-analysis. *Brain Imaging and Behavior*, *15*, 2215–2227. https://doi.org/10.1007/s11682-020-00402-7

O'Neill, A., Mechelli, A., & Bhattacharyya, S. (2019). Dysconnectivity of large-scale functional networks in early psychosis: A meta-analysis. *Schizophrenia Bulletin*, *45*, 579–590. https://doi.org/10.1093/schbul/sby094

Pantoni, L., Marzi, C., Poggesi, A., Giorgio, A., de Stefano, N., Mascalchi, M., Inzitari, D., Salvadori, E., & Diciotti, S. (2019). Fractal dimension of cerebral white matter: A consistent feature for prediction of the cognitive performance in patients with small vessel disease and mild cognitive impairment. *Neuroimage Clinical*, *24*, 101990. https://doi.org/10.1016/j.nicl.2019.101990

Paulus, M. P., Squeglia, L. M., Bagot, K., Jacobus, J., Kuplicki, R., Breslin, F. J., Bodurka, J., Morris, A. S., Thompson, W. K., Bartsch, H., & Tapert, S. F. (2019). Screen media activity and brain structure in youth: Evidence for diverse structural correlation networks from the ABCD study. *NeuroImage*, *185*, 140–153. https://doi.org/10.1016/j.neuroimage.2018.10.040

Perrier, J., Viard, A., Levy, C., Morel, N., Allouache, D., Noal, S., Joly, F., Eustache, F., & Giffard, B. (2020). Longitudinal investigation of cognitive deficits in breast cancer patients and their gray matter correlates: Impact of education level. *Brain Imaging and Behavior*, *14*, 226–241. https://doi.org/10.1007/s11682-018-9991-0

Pomares, F. B., Funck, T., Feier, N. A., Roy, S., Daigle-Martel, A., Ceko, M., Narayanan, S., Araujo, D., Thiel, A., Stikov, N., Fitzcharles, M. A., & Schweinhardt, P. (2017). Histological underpinnings of Grey matter changes in fibromyalgia investigated using multimodal brain imaging. *The Journal of Neuroscience*, *37*, 1090–1101. https://doi.org/10.1523/jneurosci.2619-16.2016

Porto, F. H. G., de Almeida, P. L., & Daffner, K. R. (2019). Teaching NeuroImages: Persistent anterograde amnesia due to sequential, bilateral vascular damage to the Papez circuit. *Neurology*, *92*, e2838–e2839. https://doi.org/10.1212/wnl.0000000000007658

Rajagopalan, V., Das, A., Zhang, L., Hillary, F., Wylie, G. R., & Yue, G. H. (2019). Fractal dimension brain morphometry: A novel approach to quantify white matter in traumatic brain injury. *Brain Imaging and Behavior*, *13*, 914–924. https://doi.org/10.1007/s11682-018-9892-2

Riccelli, R., Toschi, N., Nigro, S., Terracciano, A., & Passamonti, L. (2017). Surface-based morphometry reveals the neuroanatomical basis of the five-factor model of personality. *Social Cognitive and Affective Neuroscience*, *12*, 671–684. https://doi.org/10.1093/scan/nsw175

Sato, C., Sekiguchi, A., Kawai, M., Kotozaki, Y., Nouchi, R., Tada, H., Takeuchi, H., Ishida, T., Taki, Y., Kawashima, R., & Ohuchi, N. (2015). Postoperative structural brain changes and cognitive dysfunction in patients with breast cancer. *PLoS One*, *10*, e0140655. https://doi.org/10.1371/journal.pone.0140655

Seeley, W. W., Menon, V., Schatzberg, A. F., Keller, J., Glover, G. H., Kenna, H., Reiss, A. L., & Greicius, M. D. (2007). Dissociable intrinsic connectivity networks for salience processing and executive control. *The Journal of Neuroscience*, *27*, 2349–2356. https://doi.org/10.1523/jneurosci.5587-06.2007

Shen, C. Y., Chen, V. C., Yeh, D. C., Huang, S. L., Zhang, X. R., Chai, J. W., Huang, Y. H., Chou, M. C., & Weng, J. C. (2019). Association of functional dorsal attention network alterations with breast cancer and chemotherapy. *Scientific Reports*, *9*, 104. https://doi.org/10.1038/s41598-018-36380-6

Sung, H., Ferlay, J., Siegel, R. L., Laversanne, M., Soerjomataram, I., Jemal, A., & Bray, F. (2021). Global cancer statistics 2020: GLOBOCAN estimates of incidence and mortality worldwide for 36 cancers in 185 countries. *CA: a Cancer Journal for Clinicians*, *71*, 209–249. https://doi.org/10.3322/caac.21660

Taillibert, S., Le Rhun, E., & Chamberlain, M. C. (2016). Chemotherapy-related neurotoxicity. *Current Neurology and Neuroscience Reports*, *16*, 81. https://doi.org/10.1007/s11910-016-0686-x

Tong, T., Lu, H., Zong, J., Lv, Q., & Chu, X. (2020). Chemotherapy-related cognitive impairment in patients with breast cancer based on MRS and DTI analysis. *Breast Cancer*, *27*, 893–902. https://doi.org/10.1007/s12282-020-01094-z

Turken, A., Whitfield-Gabrieli, S., Bammer, R., Baldo, J. V., Dronkers, N. F., & Gabrieli, J. D. (2008). Cognitive processing speed and the structure of white matter pathways: Convergent evidence from normal variation and lesion studies. *NeuroImage*, *42*, 1032–1044. https://doi.org/10.1016/j.neuroimage.2008.03.057

Uddin, L. Q. (2015). Salience processing and insular cortical function and dysfunction. *Nature Reviews. Neuroscience*, *16*, 55–61. https://doi.org/10.1038/nrn3857

Uddin, L. Q., Nomi, J. S., Hébert-Seropian, B., Ghaziri, J., & Boucher, O. (2017). Structure and function of the human insula. *Journal of Clinical Neurophysiology*, *34*, 300–306. https://doi.org/10.1097/wnp.0000000000000377

Vertes, R. P., Albo, Z., & Viana Di Prisco, G. (2001). Theta-rhythmically firing neurons in the anterior thalamus: Implications for mnemonic functions of Papez's circuit. *Neuroscience*, *104*, 619–625. https://doi.org/10.1016/s0306-4522(01)00131-2

Vincent, J. L., Kahn, I., Snyder, A. Z., Raichle, M. E., & Buckner, R. L. (2008). Evidence for a frontoparietal control system revealed by intrinsic functional connectivity. *Journal of Neurophysiology*, *100*, 3328–3342. https://doi.org/10.1152/jn.90355.2008

Vossel, S., Geng, J. J., & Fink, G. R. (2014). Dorsal and ventral attention systems: Distinct neural circuits but collaborative roles. *The Neuroscientist*, *20*, 150–159. https://doi.org/10.1177/1073858413494269

Wang, E., Jia, Y., Ya, Y., Xu, J., Mao, C., Luo, W., Fan, G., & Jiang, Z. (2021). Patterns of Sulcal depth and cortical thickness in Parkinson's disease. *Brain Imaging and Behavior*, *15*, 2340–2346. https://doi.org/10.1007/s11682-020-00428-x

Wang, L., Yan, Y., Wang, X., Tao, L., Chen, Q., Bian, Y., He, X., Liu, Y., Ding, W., Yu, Y., & Qiu, B. (2016). Executive function alternations of breast cancer patients after chemotherapy: Evidence from resting-state functional MRI. *Academic Radiology*, *23*, 1264–1270. https://doi.org/10.1016/j.acra.2016.05.014

Wefel, J. S., Kesler, S. R., Noll, K. R., & Schagen, S. B. (2015). Clinical characteristics, pathophysiology, and management of noncentral nervous system cancer-related cognitive impairment in adults. *CA: a Cancer Journal for Clinicians*, *65*, 123–138. https://doi.org/10.3322/caac.21258

Wolf, R. C., Kubera, K. M., Waddington, J. L., Schmitgen, M. M., Fritze, S., Rashidi, M., Thieme, C. E., Sambataro, F., Geiger, L. S., Tost, H., & Hirjak, D. (2021). A neurodevelopmental signature of parkinsonism in schizophrenia. *Schizophrenia Research*, *231*, 54–60. https://doi.org/10.1016/j.schres.2021.03.004

Xu, W., & Südhof, T. C. (2013). A neural circuit for memory specificity and generalization. *Science*, *339*, 1290–1295. https://doi.org/10.1126/science.1229534

Yun, H. J., Im, K., Jin-Ju, Y., Yoon, U., & Lee, J. M. (2013). Automated sulcal depth measurement on cortical surface reflecting geometrical properties of sulci. *PLoS One*, *8*, e55977. https://doi.org/10.1371/journal.pone.0055977

Zhao, L., Matloff, W., Ning, K., Kim, H., Dinov, I. D., & Toga, A. W. (2019). Age-related differences in brain morphology and the modifiers in middle-aged and older adults. *Cerebral Cortex*, *29*, 4169–4193. https://doi.org/10.1093/cercor/bhy300

SUPPORTING INFORMATION

Additional supporting information may be found in the online version of the article at the publisher's website.

How to cite this article: Zhou, X., Tan, Y., Yu, H., Liu, J., Lan, X., Deng, Y., Yu, F., Wang, C., Chen, J., Zeng, X., Liu, D., & Zhang, J. (2022). Early alterations in cortical morphology after neoadjuvant chemotherapy in breast cancer patients: A longitudinal magnetic resonance imaging study. *Human Brain Mapping*, *43*(15), 4513–4528. https://doi.org/10.1002/hbm.25969